



UNIVERSITY OF TRENTO

DIPARTIMENTO DI INGEGNERIA E SCIENZA DELL'INFORMAZIONE

38123 Povo – Trento (Italy), Via Sommarive 14
<http://www.disi.unitn.it>

IMPROVING THE RECONSTRUCTION ACCURACY OF GAS- BASED NDE/NDT METHODS THROUGH A LEVEL SET APPROACH

M. Donelli, M. Benedetti, P. Rocca, M. Pastorino, A Massa

January 2011

Technical Report # DISI-11-223

Improving the Reconstruction Accuracy of GAs-Based NDE/NDT Methods through a Level Set Approach

Massimo Donelli, Manuel Benedetti, Paolo Rocca, and Andrea Massa

Department of Information and Communication Technology,
University of Trento, Via Sommarive 14, 38050 Trento, Italy
Phone: +39-0461-882057, Fax: +39-0461-882093

Email: andrea.massa@ing.unitn.it, {donelli,benedetti,rocca}@dit.unitn.it

Matteo Pastorino

Department of Biophysical and Electronic Engineering,
University of Genova, Via Opera Pia 11/A, 16145 Genoa, Italy
Phone: +39-010-3532242, Fax: +39-010-3532245
Email: pastorino@dibe.unige.it

Abstract – In the framework of nondestructive testing and evaluation (NDE/NDT), this paper deals with the problem of the detection of unknown anomalies in dielectric materials. The proposed inverse scattering approach consists of a two-step procedure aimed at firstly estimating the region-of-interest where the defect is supposed to be located and then improving the qualitative imaging (i.e., the shape and position) of the crack. In order to assess the effectiveness of the proposed approach, an illustrative result from representative numerical test cases is presented and discussed.

Keywords – NDE/NDT, Microwave Imaging, Genetic Algorithms, Level-Set.

I. INTRODUCTION

The detection of unknown defects and other anomalies in a known host domain is a topic of great interest in many industrial and biomedical applications. In this framework, electromagnetic imaging methods based on inversion procedures can play an important role [1][2][3]. In NDE and NDT, these approaches have been successfully applied for estimating with a satisfactory degree of accuracy the position and the occupation area of defects [4][5]. Despite the satisfactory results, the proposed implementations do not allow a detailed identification of the shape of targets. Thus, approximating the defective regions with rectangular shapes turns out to be critical especially in those applications (e.g., biomedical diagnosis) where an accurate knowledge of the size as well as of the contour of the defect may be very important. Therefore, this paper proposes a two-step procedure aimed at increasing the accuracy in detecting the contour and consequently the occupation area of a given defect inside a known structure.

At the first step, starting from the knowledge of the scattered field with and without the defect, the detection problem is reformulated in terms of an inverse scattering one and successively recast as the global optimization of a suitably-defined cost function. In order to determine the region-of-interest (RoI) where the defect is supposed to be located, the cost function is minimized by means of a global optimization technique based on the use of a hybrid-coded genetic algorithm (GA) [6]. The second step is aimed at refining the reconstruction of the defect by means of a shape-based optimization technique characterized by the evolution of a Level Set function [7].

The paper is organized as follows. A short mathematical formulation describes the electromagnetic scenario in terms of descriptive inverse scattering relationships (Sect. II). Then, the proposed two-step strategy is presented focusing on the integration between the GA-based algorithm and the methodology based on the shape deformation (Sect. III). Finally, the effectiveness of the proposed approach is discussed (Sect. IV) and some conclusions are drawn.

II. PROBLEM FORMULATION

Let us consider a two-dimensional scenario $[r = (x, y), r \text{ being the position vector}]$ where a cylindrical region D is characterized by a relative permittivity ε_D and a conductivity σ_D . A homogeneous defect (or crack) characterized by

unknown position $\underline{r}_c = (x_c, y_c)$ and shape Ω lies in D . Such a scenario is illuminated by V electromagnetic TM plane waves with an incident field $\underline{E}_{inc}^v(\underline{r}) = E_{inc}^v(\underline{r})\hat{z}$. The induced electromagnetic field, $\underline{E}_{tot}^v(\underline{r})$, is given by

$$\underline{E}_{tot}^v(\underline{r}) = \underline{E}_{inc}^v(\underline{r}) + \iint_D \tau(\underline{r}') \underline{E}_{tot(c)}^v(\underline{r}') G_0(\underline{r}'/\underline{r}) d\underline{r}' \quad (1)$$

where G_0 is the free-space Green's function and $\tau(\underline{r}) = \varepsilon(\underline{r}) - 1 - j \frac{\sigma(\underline{r})}{2\pi f \varepsilon_0}$ is the object function, f being the working frequency. The arising scattering phenomena can be modeled in an equivalent fashion by assuming that a differential equivalent current density defined in the region Ω radiates in an inhomogeneous space. Thus, equation (1) can be rewritten as follows [8]

$$\underline{E}_{tot}^v(\underline{r}) = \underline{E}_{inc(cf)}^v(\underline{r}) + \iint_{\Omega} \tau_{\Omega}(\underline{r}') \underline{E}_{tot(c)}^v(\underline{r}') G_1(\underline{r}'/\underline{r}) d\underline{r}' \quad (2)$$

where $G_1(\underline{r}'/\underline{r})$ is the inhomogeneous Green's function and $\underline{E}_{inc(cf)}^v(\underline{r})$ is the total electric field in the scenario without defect (i.e., the crack-free scenario) given by

$$\underline{E}_{inc(cf)}^v(\underline{r}) = \underline{E}_{inc}^v(\underline{r}) + \iint_D \tau_D \underline{E}_{inc(cf)}^v(\underline{r}') G_0(\underline{r}'/\underline{r}) d\underline{r}' \quad (3)$$

In equation (2), $\tau_{\Omega}(\underline{r})$ is the differential object function defined as follows

$$\tau_{\Omega}(\underline{r}) = \begin{cases} (\varepsilon_c - \varepsilon_D) - j \frac{(\sigma_c - \sigma_D)}{2\pi f \varepsilon_0} & \text{if } \underline{r} \in \Omega \\ 0 & \text{if } \underline{r} \notin \Omega \end{cases} \quad (4)$$

where ε_c and σ_c are the relative permittivity and the conductivity characterizing the defective region Ω .

In order to numerically deal with the scattering equation (3), the region D is partitioned into N sub-domains following the Richmond's method [9]. Accordingly, the Green's inhomogeneous operator is discretized and stored in a $N \times N$ matrix $[G_i]$. Moreover, let us indicate with P the number of sub-domains occupied by the defective region Ω and let us express equation (3) in matrix form

$$[E_{tot}^v] = [E_{inc(cf)}^v] + [G_{1,\Omega}] \tau_{\Omega} [E_{tot(c)}^v] \quad (5)$$

where:

- $[E_{inc(cf)}^v]$ and $[E_{tot}^v]$ are complex arrays of size $N \times 1$ whose entries are the total electric field samples in the crack-free and perturbed configuration, respectively;
- $[E_{tot(c)}^v]$ is a $P \times 1$ complex matrix containing the total field for the unperturbed scenario;
- $[\tau_{\Omega}]$ is a $P \times P$ diagonal matrix where the P values of the differential object function $\tau_{\Omega}(\underline{r})$ are stored;
- $[G_{1,\Omega}]$ is a $N \times P$ complex matrix obtained from $[G_i]$ selecting the P columns related to the position p ($p = 1, \dots, P$) of the defective pixels of Ω .

In order to retrieve the unknown position and shape of the crack Ω , let us consider a two-step procedure based on the detection of the RoI where the support of the crack is roughly estimated [4] and a successive shape-optimization refinement strategy [10].

As far as the first step is concerned, the region-of-interest is approximated by a rectangular homogeneous domain R properly parameterized. Instead of reconstructing the permittivity profile in the whole region D , let us describe the region-of-interest with the coordinates of the center $\underline{r}_R = (x_R, y_R)$, its length L_R , side W_R , and orientation θ_R . Thus, according to the inhomogeneous space formulation, the differential object function of the region-of-interest R becomes

$$\tau_R(\underline{r}) = \begin{cases} \tau_{\Omega}(\underline{r}) & \text{if } X \in \left[-\frac{L_R}{2}, \frac{L_R}{2}\right] \text{ and } Y \in \left[-\frac{W_R}{2}, \frac{W_R}{2}\right] \\ 0 & \text{otherwise} \end{cases} \quad (6)$$

with $X = (x - x_R)\cos\theta_R + (y - y_R)\sin\theta_R$ and $Y = (x - x_R)\sin\theta_R + (y - y_R)\cos\theta_R$.

Since the problem unknowns are both the object function (6) and the total electric field distribution, the following set of parameters is looked for

$$\chi = [x_R, y_R, L_R, W_R, \theta_R, \{E_{tot(c),p}^v; p=1, \dots, P\}] \quad (7)$$

where $\{E_{tot(c),p}^v; p=1, \dots, P\}$ represent the total field samples in the region R approximating the defect Ω .

In order to retrieve the optimal solution χ_{opt} , the inverse scattering problem is solved by means of an optimization procedure. Starting from the information collected in the observation domain O [i.e., the total field with the defect $E_{tot}^v(r_m)$ and without the defect $E_{tot(cf)}^v(r_m)$, $m=1, \dots, M$] and in the investigation domain D [i.e., $E_{inc}^v(r_n)$, $n=1, \dots, N$], the cost function quantifying the mismatching between estimated and measured scattering data, is minimized

$$\Theta_1(\chi) = \left\{ \frac{\| [E_{tot}^v] - [E_{tot(cf)}^v] - [G_{1,R}] \tau_R [E_{tot(c)}^v] \|_O^2}{\| [E_{tot}^v] - [E_{inc}^v] \|_O^2} \right\} + \left\{ \frac{\| [E_{tot(cf)}^v] + [E_{tot}^v] - [G_{1,R}] \tau_R [E_{tot(c)}^v] \|_D^2}{\| [E_{inc}^v] \|_D^2} \right\} \quad (8)$$

according to the Inhomogeneous Green's function Approach (IGA) [4]. More in detail, Q trial solutions $\underline{\chi}^j = \{\chi_q^j, q=1, \dots, Q\}$ are randomly initialized ($j=0$, j being the iteration index) and an iterative procedure is applied until a stopping criterion holds true ($j = J_{max}$ or $\Theta_1(\chi_{opt}) < \gamma_{th}$, $\chi_{opt} = \arg\{\min_{q=1, \dots, Q} [\min_{j=1, \dots, J_{max}} \Theta_1(\chi_q^j)]\}$). The set of operations performed at the j -th iteration can be summarized as follows:

- the iteration index is updated ($j = j + 1$);
- a set of genetic operators is applied to get the j -th population [$\underline{\chi}^j = \mathfrak{Z}(\underline{\chi}^{j-1})$];
- the best trial solution at the iteration j is found ($\chi_{opt}^j = \arg\{\min_{q=1, \dots, Q} [\Theta_1(\chi_q^j)]\}$).

As far as the hybrid genetic operators $\mathfrak{Z}(\cdot)$ are concerned, the *crossover*, *elitism*, *selection* and *mutation* described in [4] are adopted.

The GA-based optimization returns a set of parameters defining the region-of-interest. They are

$$\chi_{opt} = [\hat{x}_R, \hat{y}_R, \hat{L}_R, \hat{W}_R, \hat{\theta}_R, \{\hat{E}_{tot(c),p}^v; p=1, \dots, P\}] \quad (9)$$

where the superscript $\hat{\cdot}$ denotes the estimated values.

The second step of the approach is aimed at refining the estimation of the quantitative descriptors of the defect starting from the knowledge acquired at the first step. More in detail, a level-set-based strategy is employed in order to exploit such an available *a-priori* information on the unknown (i.e., the defect is an homogeneous region and lies in the RoI). Such an algorithm is initialized by defining an initial trial shape Ψ_0 centered at \hat{L}_R and with radius equal to $\rho = \alpha \sqrt{(\hat{L}_R/2)^2 + (\hat{W}_R/2)^2}$, α being a parameter to be empirically chosen. Then, the Level Set ϕ_0 is computed according to an oriented distance function [10] and the following sequence of iterative steps is performed:

- the fitness of the trial shape Ψ_k is evaluated using the following metric

$$\Theta_2(\tau_k) = \left\{ \frac{\| [E_{meas}^v] - [E^v(\tau_k)] \|_O^2}{\| [E_{meas}^v] \|_O^2} \right\} \quad (10)$$

where:

- $[E_{meas}^v]$ is the scattered field array ($[E_{meas}^v] = [E_{tot}^v] - [E_{inc}^v]$);
- $[E^v(\tau_k)]$ is the array whose entries are the samples of the field scattered by a defect with shape Ψ_k in a domain whose object function $\tau_k(r_n)$ is equal to $\tau_C = \varepsilon_C - 1 - j \frac{\sigma_C}{2\pi f \varepsilon_0}$ if $\phi_k \leq 0$ and τ_D otherwise;

- b) a convergence check is performed in order to stop the level-set-based refinement step. Accordingly, the reconstruction procedure is arrested if a maximum number of iteration is reached ($k < K_{\max}$) or if the misfit (10) is lower than a fixed threshold ($\Theta_2(\tau_k) < \gamma_{th}$);
- c) by solving an Hamilton-Jacobi equation, the level set function ϕ_k is updated

$$\frac{\phi_{k+1}(\underline{r}_n) - \phi_k(\underline{r}_n)}{\Delta t} = \eta_k(\underline{r}_n) H\{\phi_k(\underline{r}_n)\} \quad (12)$$

where $H\{\phi_k(\underline{r}_n)\}$ is the numerical Hamiltonian [10][11], Δt is the time-step, and $\eta_k(\underline{r}_n)$ is a smoothed velocity computed as follows

$$\eta_k(\underline{r}_n) = \begin{cases} v_k(\underline{r}_n) & \text{if } \|\underline{r}_n - \hat{\underline{r}}_R\| \leq \rho \\ v_k(\underline{r}_n) \frac{\rho}{\beta \|\underline{r}_n - \hat{\underline{r}}_R\|} & \text{if } \|\underline{r}_n - \hat{\underline{r}}_R\| > \rho \end{cases} \quad (11)$$

where β is a parameter to be chosen heuristically;

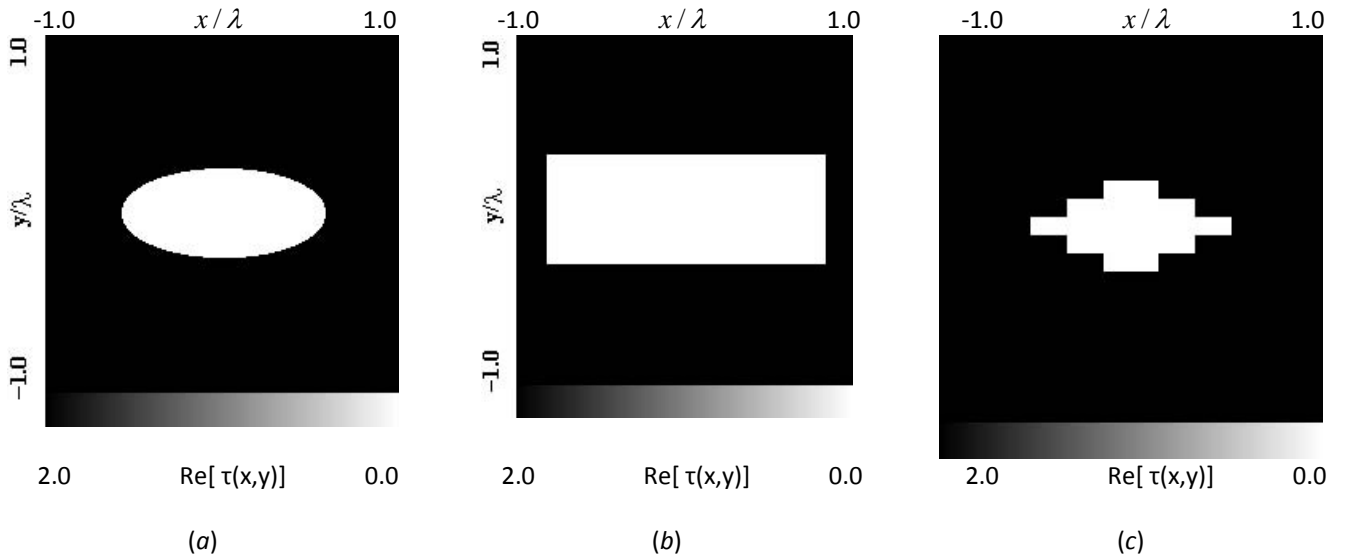


Fig.1. Reconstruction of an elliptic defect centered in a host medium characterized by $\epsilon_D = 2.0$. Actual profile (a). Retrieved distribution at (b) the first step and at (c) the second step of the inversion.

- d) the iteration index is updated ($k = k + 1$).

When the level-set-based process terminates, the distribution $\tau_{opt}(\underline{r}_n)$, which is a function of ϕ_{opt} at the iteration k_{opt} , gives an estimate of the actual permittivity profile.

III. NUMERICAL RESULTS

In order to assess the effectiveness of the proposed strategy, a selected representative result is reported and analyzed. Let us consider an unknown elliptical void that lies in a square lossless homogeneous host medium of side $L_D = 2.0\lambda$ and characterized by a dielectric permittivity equal to $\epsilon_D = 2.0$. $V = 4$ plane waves coming from orthogonal angular directions probes such a scenario and the scattered samples are collected at $M = 50$ measurement points. Moreover, in order to simulate realistic environmental conditions, a noise of Gaussian-type and characterized by a fixed signal-to-noise ratio (SNR) of 30 dB has been added to the scattering data.

Fig. 1(a) shows the actual distribution of the object function in the scenario under test. As it can be observed [Fig. 1(b)], the region of interest retrieved at the end of the first step contains the support of the defect, but its shape largely overestimates the actual shape of the crack. In order to improve the qualitative imaging, the level-set-based procedure (second step) is applied. The final reconstruction is shown in Fig. 1(c). The unknown defect is rightfully located ($\hat{x}_c = 0.01\lambda_0$, $\hat{y}_c = -0.05\lambda_0$) and the extension of the actual shape is estimated with a good degree of accuracy.

In dealing with the same configuration, the effects of the variation of the noise level have been evaluated, as well. Towards this purpose, the signal-to-noise ratio has been varied from 30 up to 5 dB. Tab. I gives the values of the error figures (δ - localization error, Δ - area error, and ε_{tot} - total reconstruction error [5]) in correspondence with the different SNRs. As it can be noticed, the two-step method seems to be reasonably stable with respect to the noise.

SNR [dB]	δ	Δ	ε_{tot}
30	$0.01 \lambda_0$	$0.03 \lambda_0$	0.07
20	$0.09 \lambda_0$	$0.08 \lambda_0$	0.09
10	$0.11 \lambda_0$	$0.10 \lambda_0$	0.12
5	$0.13 \lambda_0$	$0.18 \lambda_0$	0.15

Tab.1. Elliptic void. Error figures versus signal to noise ratio.

CONCLUSIONS

In this work, an innovative two-steps procedure for NDE/NDT applications has been proposed and preliminary assessed. The method consists of a first phase where the region of interest, to which the defect belongs, is estimated and a successive refinement process aimed at enhancing the qualitative imaging of the defective region. The effectiveness and robustness of such an approach have been evaluated by considering a selected set of synthetic experiments. Certainly, further analyses are needed, but some features of the approach seem to be very attractive for practical applications in biomedical imaging.

REFERENCES

- [1] J. C. Bolomey, "Recent European developments in active microwave imaging for industrial, scientific and medical applications," *IEEE Trans. Microwave Theory Tech.*, vol. 37, pp. 2109–2117, June 1989.
- [2] R. Zoughi, *Microwave Nondestructive Testing and Evaluation*. The Netherlands: Kluwer Academic, 2000.
- [3] K. Meyer, K. J. Langenberg, and R. Schneider, "Microwave imaging of defects in solids," in Proc. 21st Annual Review of *Progress in Quantitative NDE*, Snowmass Village, CO, July 31-Aug. 5 1994.
- [4] S. Caorsi, A. Massa, and M. Pastorino, "A crack identification microwave procedure based on a genetic algorithm for nondestructive testing," *IEEE Trans. Antennas Propagat. Magazine*, vol. 37, pp. 7-15, 1995.
- [5] S. Caorsi, A. Massa, M. Pastorino, and M. Donelli, "Improved microwave imaging procedure for nondestructive evaluations of two-dimensional structures," *IEEE Trans. Antennas Propagat.*, Vol. 52, pp. 1386-1397, Jun. 2004.
- [6] Y. Rahmat Samii and E. Michielssen, *Electromagnetic Optimization by Genetic Algorithms*. New York: Wiley 1999.
- [7] O. Dorn and D. Lesselier, "Level set methods for inverse scattering", *Inverse Problems*, 22, 2006, pp. R67-R131.
- [8] S. Caorsi, G. L. Gagnani, M. Pastorino, and M. Rebagliati, "A model-driven approach to microwave diagnostics in biomedical applications," *IEEE Trans. Microwave Theory Tech.*, vol. 44, pp. 1910-1920, 1996.
- [9] J. H. Richmond, "Scattering by a dielectric cylinder of arbitrary cross-section shape," *IEEE Trans. Antennas Propagat.*, vol. AP-13, pp. 334-341, 1965.
- [10] A. Litman, D. Lesselier, and F. Santosa, "Reconstruction of a two-dimensional binary obstacle by controlled evolution of a level-set," *Inverse Problem*, Vol. 14, pp. 685-706, 1998.
- [11] S. Osher and J. A. Sethian "Fronts propagating with curvature-dependent speed: algorithms based on Hamilton–Jacobi formulations," *J. Comput. Phys.* 79, pp. 12–49, 1988.